Computers and Concrete, Vol. 9, No. 3 (2012) 195-214

DOI: http://dx.doi.org/10.12989/cac.2012.9.3.195

Investigation of effectiveness of double concave friction pendulum bearings

Sevket Ates*

Department of Civil Engineering, Karadeniz Technical University, Trabzon, 61080, Turkey

(Received July 13, 2010, Revised April 8, 2011, Accepted May 11, 2011)

Abstract. This paper presents the investigation of the stochastic responses of seismically isolated bridges subjected to spatially varying earthquake ground motions including incoherence, wave-passage and site-response effects. The incoherence effect is examined by considering Harichandran and Vanmarcke coherency model. The effect of the wave-passage is dealt with various wave velocities in the response analysis. Homogeneous firm, medium and soft soil conditions are selected for considering the site-response effect where the bridge supports are constructed. The ground motion is described by filtered white noise and applied to each support points. For seismic isolation of the bridge, single and double concave friction pendulum bearings are used. Due to presence of friction on the concave surfaces of the isolation systems, the equation of motion of is non-linear. The non-linear equation of motion is solved by using equivalent linearization technique of non-linear stochastic analyses. Solutions obtained from the stochastic analyses of non-isolated and isolated bridges to spatially varying earthquake ground motions compared with each other for the special cases of the ground motion model. It is concluded that friction pendulum systems having single and double concave surfaces have important effects on the stochastic responses of bridges to spatially varying earthquake ground motions.

Keywords: seismic isolation; highway bridge; spatially varying ground motions; stochastic analysis; equivalent linearization technique.

1. Introduction

Base isolation of structures is a viable solution for earthquake protection. Using base isolation, responses of structures such as buildings, bridges, tanks and pipelines are shifted to a higher fundamental period. Base isolations have been commonly used in the construction of new structures and retrofit of existing structures during the last years. Two of the base isolation bearings are that of single and double concave friction pendulum (SCFP and DCFP). The bearings are innovative and viable isolation bearings that are becoming a more widespread application for the earthquake protection of structures. While the SCFP bearings have one concave surface, the DCFP consists of two concave surfaces and an articulated slider covered by a Teflon-based high bearing capacity composite material. The concave surfaces may be the same radii of curvature in latter isolation bearing. Also, the coefficient of friction on the two concave surfaces may be the same or different. Experimental and analytical results on the behaviour of a system having concave surfaces of both equal and unequal radii and both equal and unequal coefficient of friction at the upper and lower sliding surfaces were presented by Tsai *et al.* (2006). Constantinou (2004), Fenz and Constantinou

* Corresponding author, Assistant Professor, E-mail: sates@ktu.edu.tr

(2006) described the principles of operation of the DCFP bearing and presented the development of the force-displacement relationship based on considerations of equilibrium. The theoretical force-displacement relationship was verified through characterization testing of bearings with sliding surfaces having the same and then different radii of curvature and coefficients of friction. Also, practical considerations for analysis and design of DCFP bearings were presented. Hyakuda *et al.* (2001) presented the description and observed response of a seismically isolated building in Japan which utilized DCFP bearings. Zayas *et al.* (1989) introduced one of the most effective sliding isolation systems, namely the friction pendulum system namely SCFP, which utilizes friction to dissipate the transmitted energy to the structure.

The dynamic responses of extended structures like bridges, pipelines and dams are significantly affected by spatially varying earthquake ground motions. The earthquake response analysis of long span non-isolated bridges subjected to spatially varying earthquake ground motions were investigated by many researchers (Harichandran and Wang 1988, Zerva 1991, Kiureghian and Neuenhofer 1991, Harichandran *et al.* 1996). Lou and Zerva (2005) investigated the effects of spatially varying earthquake ground motions on the seismic response of a skewed, multi-span and RC highway bridge. Soyluk and Dumanoglu (2004) carried out stochastic analysis of non-isolated cable-stayed bridges for delayed support excitations and concluded that any seismic analysis of even moderately long span non-isolated cable-stayed bridges requires the consideration of the wave-passage effects. Soyluk *et al.* (2004) presented various random vibration and deterministic analyses of non-isolated cable-stayed bridges to asynchronous ground motion. It was found that the structural response values show important amplifications depending on the decreasing ground motion wave velocities. Ates *et al.* (2005, 2006, 2009) studied stochastic response of isolated bridges by friction pendulum systems to spatially varying earthquake ground motions and reported that friction pendulum systems have important effects on the stochastic responses of bridges to spatially varying earthquake ground motions.

A new procedure for simulating the tunnel response under spatially varying ground motion was developed by Parka *et al.* (2009). The procedure utilizes the longitudinal displacement profile, which is developed from spatially variable ground motion time histories. The longitudinal displacement profile is used to perform a series of pseudo-static three-dimensional finite-element analyses. Results of the analyses show that the spatially variable ground motion causes longitudinal bending of the tunnel and can induce substantial axial stress on the tunnel lining. The effect can be significant at boundaries at which the properties of the ground change in the longitudinal direction. Konakli and Der Kiureghian (2011) introduced a generalized formulation of the multiple support response spectrum method by accounting for the quasi-static contributions of truncated modes. The effects of differential support motions including the influence of spatially varying soil conditions on the quasi-static, dynamic and total responses were examined.

The effects of the uniform and spatially varying ground motions on the stochastic response of fluid-structure interaction system during an earthquake were investigated by using the displacement based fluid finite elements (Bilici *et al.* 2009). It was concluded that spatially varying earthquake ground motions have important effects on the stochastic response of fluid-structure interaction systems.

It will be seen from the literature review above that the importance of spatially varying earthquake ground motions on the non-isolated bridges were investigated by many researches. As a result of these studies, it is highlighted that spatially varying earthquake ground motions including incoherence, wave passage and site-response effects should be taken into account separately and altogether in the analyses. The effects of spatially varying earthquake ground motions on the isolated bridges with the DCFP bearings have not been comprehensively investigated up to date. For this reasons, the focus of this study is to investigate the effectiveness of the spatially varying earthquake ground motion on the stochastic response of isolated multi-span continuous bridges with the DCFP bearings and compared with the SCFP bearings.

2. Double concave friction pendulum bearings

The double concave friction pendulum (DCFP) bearings are made of two concave surfaces which are named as upper and lower and shown in Fig. 1 (Constantinou 2004, Fenz and Constantinou 2006). The concave surfaces may be the same radii of curvature. Also, the coefficient of friction on the two concave surfaces may be the same or not equal. The maximum displacement capacity of the bearing is 2*d*, where *d* is the maximum displacement capacity of a single concave surface in Fig. 1. Note that due to rigid body and relative rotation of the slider, the displacement capacity is actually slightly different than 2*d*. The force-displacement relationship for the DCFP bearing is given by the following equation

$$F = \left(\frac{W}{R_1 - h_1 + R_2 - h_2}\right)v_b + \left(\frac{F_{f1}(R_1 - h_1) + F_{f2}(R_2 - h_2)}{R_1 - h_1 + R_2 - h_2}\right) \tag{1}$$

where W is the vertical load, R_1 and R_2 are radii of the two concave surfaces, h_1 and h_2 are the part

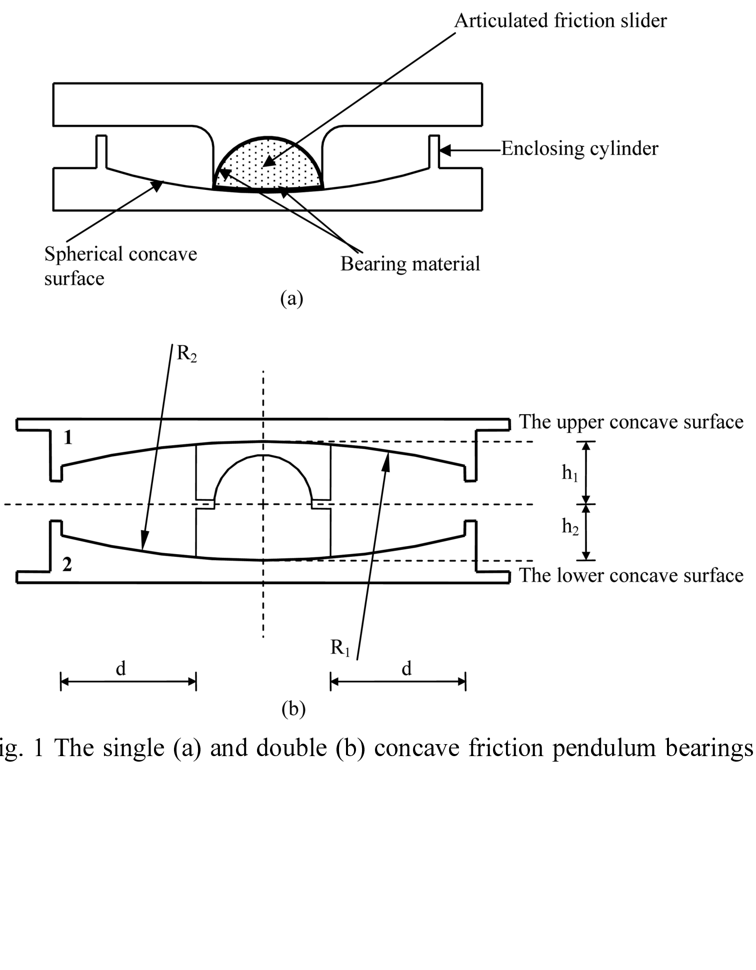

Fig. 1 The single (a) and double (b) concave friction pendulum bearings

heights of the articulated slider, V_b is the total displacement (bearing displacement) and the sum of the displacements on the upper and lower surfaces

$$v_b = 2d = v_{b1} + v_{b2} \tag{2}$$

herein v_{b1} and v_{b2} are the displacements of the slider on the upper and the lower concave surfaces, respectively, and the individual displacements on each sliding surfaces are

$$v_{b1} = \left(\frac{F-F_{f1}}{W}\right)(R_1-h_1) \tag{3}$$

$$v_{b2} = \left(\frac{F-F_{f2}}{W}\right)(R_2-h_2) \tag{4}$$

in Eqs. (3) and (4), F_{f1} and F_{f2} are the friction forces on the concave surfaces 1 and 2, respectively. The forces are given by

$$F_{f1} = \mu_1 W \mathrm{sgn}(\dot{v}_{b1}) \tag{5}$$

$$F_{f2} = \mu_2 W \mathrm{sgn}(\dot{v}_{b2}) \tag{6}$$

where μ_1 and μ_2 are the coefficient of friction on the concave surfaces 1 and 2, respectively; $\dot{v}_{b1}$ and $\dot{v}_{b2}$ are sliding velocities at upper and lower surfaces, respectively; sgn (.) denotes signum function. Most applications of the DCFP bearings will likely utilize concave surfaces of equal radii, namely, $R_1 = R_2$. Parts height of the articulated slider h_1 and h_2 are nearly equal in most cases.

In Eq. (1), the first is the stiffness of the pendulum component (spring forces) and the second is the stiffness of the friction component. The natural period of vibration is given by following equation

$$T = 2\pi\sqrt{\frac{R_1+R_2-h_1-h_2}{g}} = 2\pi\sqrt{\frac{R_e}{g}} \tag{7}$$

where g is the acceleration of gravity; R_e is the effective radius of curvatures. Eq. (7) shows that the natural period of vibration is independent of mass, but it is controlled by the selection of the radius of the spherical concave surfaces. In this study, the period of the isolation system is calculated as 2.75 sec by depending on the radii of the two concave surfaces. The important parameter is employed as $R_e = R_1+R_2-h_1-h_2 = 1.88$ m. The lateral restoring stiffness of the DCFP bearing (spring forces) is given by following equation

$$k_b = \frac{W}{R_1+R_2-h_1-h_2} \tag{8}$$

It is also shown in Eq. (8) that the stiffness of the pendulum depends on weight carried by bearing. The coefficient of the friction of the two concave surfaces depend on bearing pressure and given by Eq. (9)

$$\mu_{1,2} = f_{\max} - (f_{\max} - f_{\min})e^{(a|\dot{v}_b|)} \tag{9}$$

where $f_{\max}$ and $f_{\min}$ are the maximum and minimum mobilized coefficients of friction, respectively; and a is a parameter that controls the variation of the coefficient with the velocity of sliding. Thus, the effective coefficient of friction equal to the average of μ_1 and μ_2, and is given by

$$\mu_e = \frac{\mu_1(R_1 - h_1) + \mu_2(R_2 - h_2)}{R_1 + R_2 - h_1 - h_2} \tag{10}$$

In this study, $R_1 - h_1 = R_2 - h_2 = 0.94$ m and μ_e is calculated as 0.05 by Eq. (10) due to variability in properties $\mu_1 = 0.045$ and $\mu_2 = 0.055$.

3. Single concave friction pendulum

Single concave friction pendulum (SCFP) proposed by Zayas *et al.* (1989) is chosen as a sliding bearing system namely friction pendulum system shifting the natural period of the supported structure. The natural period of vibration is given by following equation

$$T = 2\pi\sqrt{\frac{R}{g}} \tag{11}$$

where R is the radius of spherical concave surface, and g is the acceleration of gravity. Eq. (11) shows that the natural period of vibration is independent of mass, but it is controlled by the selection of the radius of the spherical concave surface. The force-displacement relationship of the SCFP in any direction may be given by the expression

$$F = \frac{W}{R}v_b + \mu_s W \mathrm{sgn}(\dot{v}_b) \tag{12}$$

where W, R, v_b, μ_s and $\dot{v}_b$ are the total weight carried by the SCFP, the radius of spherical concave surface, the sliding displacement, the coefficient of friction on the sliding surface and the sliding velocity, respectively; sgn ( ) is the signum function. In Eq. (12), the first is the pendulum component and the second is the friction component. The lateral restoring stiffness of the bearing is given by following equation

$$k_b = \frac{W}{R} \tag{13}$$

It is also shown in Eq. (13) that the stiffness of the pendulum depends on weight carried by bearing.

4. Governing equation of motion

The equation of motion of a structural system can be written as

$$\begin{bmatrix} \mathbf{M}_{rr} & \mathbf{M}_{rg} \\ \mathbf{M}_{gr} & \mathbf{M}_{gg} \end{bmatrix} \begin{Bmatrix} \ddot{\mathbf{v}}_r \\ \ddot{\mathbf{v}}_g \end{Bmatrix} + \begin{bmatrix} \mathbf{C}_{rr} & \mathbf{C}_{rg} \\ \mathbf{C}_{gr} & \mathbf{C}_{gg} \end{bmatrix} \begin{Bmatrix} \dot{\mathbf{v}}_r \\ \dot{\mathbf{v}}_g \end{Bmatrix} + \begin{bmatrix} \mathbf{K}_{rr} & \mathbf{K}_{rg} \\ \mathbf{K}_{gr} & \mathbf{K}_{gg} \end{bmatrix} \begin{Bmatrix} \mathbf{v}_r \\ \mathbf{v}_g \end{Bmatrix} = \begin{Bmatrix} \mathbf{R} \\ \mathbf{0} \end{Bmatrix} \tag{14}$$

where [**M**], [**C**] and [**K**] are the mass, damping and stiffness matrices, respectively; $\{\ddot{\mathbf{v}}\}, \{\dot{\mathbf{v}}\}$ and $\{\mathbf{v}\}$ are vectors of total accelerations, velocities and displacements, respectively and $\{\mathbf{R}\}$ is a vector of reaction force. The degrees of freedom can be defined as known and unknown. The known degrees of freedom are associated with those of the structure-foundation interface. The unknowns are related to degrees of freedom of the structure. The former degrees of freedom will be denoted henceforth as the vector $\mathbf{v}_g$, and the latter as $\mathbf{v}_r$. Here, the subscript g denotes the ground degrees of freedom and r denotes the response degrees of freedom (Harichandran *et al.* 1996, Ates *et al.* 2005, 2006).

5. Stochastic response

The variance of the ith total response is expressed as (Harichandran *et al.* 1996)

$$\sigma_{z_i}^2 = \sigma_{z_1}^{2qs} + \sigma_{z_1}^{2d} + 2Cov(z_i^{qs}, z_i^d) \tag{15}$$

in which $\sigma_{z_1}^{2qs}$ is the variance of the ith quasi-static response component; $\sigma_{z_i}^{2d}$ is the variance of the ith dynamic response component and $Cov(z_i^{qs}, z_i^d)$ is the covariance between the ith quasi-static and dynamic components. The variance of the ith quasi-static component can be written as

$$\sigma_{z_i}^{2qs} = \int_{-\infty}^{\infty} S_{z_i}^{qs}(\omega)d\omega = \sum_{l=1}^{r}\sum_{m=1}^{r} A_{il}A_{im}\int_{-\infty}^{\infty}\frac{1}{\omega^4}S_{\ddot{v}_{g_l}\ddot{v}_{g_m}}(\omega)d\omega \tag{16}$$

in which $S_{z_i}^{qs}(\omega)$ is the ith quasi-static component of the spectral density function of the structural response; r is the number of restrained degrees of freedom; $S_{\ddot{v}_{g_l}\ddot{v}_{g_m}}(\omega)$ is the cross-spectral density function of accelerations between supports l and m; and A_{il} and A_{im} are equal to static displacements for unit displacements assigned to each support points. The variance of the ith dynamic response component may be defined as

$$\sigma_{z_i}^{2d} = \int_{-\infty}^{\infty} S_{z_i}^{d}(\omega)d\omega = \sum_{j=1}^{n}\sum_{k=1}^{n}\sum_{l=1}^{r}\sum_{m=1}^{r} \psi_{ij}\psi_{ik}\Gamma_{lj}\Gamma_{mk}\int_{-\infty}^{\infty}H_j(-\omega)H_k(\omega)S_{\ddot{v}_{g_l}\ddot{v}_{g_m}}(\omega)d\omega \tag{17}$$

where $S_{z_i}^{qs}(\omega)$ is the ith dynamic component of the spectral density function of the structural response; $H(\omega)$ is the frequency response function; n is the number of free degrees of freedom; ψ is the eigenvectors and Γ is the modal participation factor. The covariance of the ith quasi-static and dynamic components is obtained as

$$Cov(z_i^{qs}, z_i^d) = -\sum_{j=1}^{n}\sum_{l=1}^{r}\sum_{m=1}^{r} \psi_{ij}A_{il}\Gamma_{mj}\left(\int_{-\infty}^{\infty}\frac{1}{\omega^2}H_j(\omega)S_{\ddot{v}_{g_l}\ddot{v}_{g_m}}(\omega)d\omega\right) \tag{18}$$

The most important parameters in stochastic analysis are mean of maximum value and its standard deviation. The maximum value can be expressed as

$$\mu = p\sigma_z \tag{19}$$

The standard deviation of the mean of maximum value is defined as

$$\sigma = q\sigma_z \tag{20}$$

where p and q are peak factors which are functions of the time of the motion and mean zero-crossing rate, respectively.

6. Spatially varying ground motion

The cross-spectral density function of the earthquake ground motion, between support points l and m is expressed as (Harichandran *et al.* 1996)

$$S_{\ddot{v}_{g_l}\ddot{v}_{g_m}}(\omega) = \gamma_{lm}(\omega)\sqrt{S_{\ddot{v}_{g_l}\ddot{v}_{g_l}}(\omega)S_{\ddot{v}_{g_m}\ddot{v}_{g_m}}(\omega)} \tag{21}$$

where $\gamma_{lm}(\omega)$ denotes the coherency function. The power spectral density function is assumed to be of the following form suggested by Clough and Penzien (1993)

$$S_{\ddot{v}_g}(\omega) = S_o\left[\frac{\omega_f^4+4\xi_f^2\omega_f^2\omega^2}{(\omega_f^2-\omega^2)^2+4\xi_f^2\omega_f^2\omega^2}\cdot\frac{\omega^4}{(\omega_g^2-\omega^2)^2+4\xi_g^2\omega_g^2\omega^2}\right] \tag{22}$$

are the frequency responses of first and second filters representing characteristics of the layers of soil medium above the rock bed; S_o is the amplitude of the white-noise process; ω_f and ξ_f are the resonant frequency and damping of the first filter, and ω_g and ξ_g are those quantities of the second filter.

In this paper, S_o is obtained for each soil type by equating the variance of the ground acceleration to the variance of the SKR090 component of Kocaeli, Turkey, earthquake recorded at Sakarya station in 1999. The calculated values of the intensity parameter for each soil type are shown in Table 1. Homogeneous firm, medium and soft soil conditions are used for the non-isolated and isolated bridge supports and the filter parameters for these soil conditions which are proposed Der Kiureghian and Neuenhofer (1991) are also utilised as shown in Table 1. The earthquake is given in Fig. 2(a); its power spectral density function and its acceleration spectral density function for different soil types are given in Figs. 2(b) and 2(c), respectively.

The coherency function is dimensionless and of complex value. The coherency function is defined as

$$\gamma_{lm}(\omega) = |\gamma_{lm}(\omega)|^i\gamma_{lm}(\omega)^w\gamma_{lm}(\omega)^s \tag{23}$$

where $|\gamma_{lm}(\omega)|^i$ characterises the incoherence effect, $\gamma_{lm}(\omega)^w$ indicates the complex valued wave-passage effect and $\gamma_{lm}(\omega)^s$ denotes the complex valued site-response effect.

For the incoherence effect, resulting from reflections and refractions of waves through the soil during their propagation, an extensively used model is considered. The model proposed by Harichandran and Vanmarcke (1986) is defined as

$$|\gamma_{lm}(\omega)|^i = A\ \exp\left[-\frac{2d_{lm}}{\alpha\theta(\omega)}(1-A+\alpha A)\right]+(1-A)\exp\left[-\frac{2d_{lm}}{\theta(\omega)}(1-A+\alpha A)\right] \tag{24}$$

$$\theta(\omega) = k\left[1+\left(\frac{\omega}{2\pi f_o}\right)^b\right]^{-\frac{1}{2}} \tag{25}$$

where d_{lm} is the distance between support points l and m; A, α, k, f_o and b are 0.736, 0.1470, 5210,

Table 1 Filter and intensity parameter of filtered white-noise process for different soil types

Soil type	ω_f (rad/s)	ξ_f	ω_g (rad/s)	ξ_g	S_o (m^2/s^3)
Firm	15.0	0.6	1.5	0.6	0.000464
Medium	10.0	0.4	1.0	0.6	0.000689
Soft	5.0	0.2	0.5	0.6	0.000968

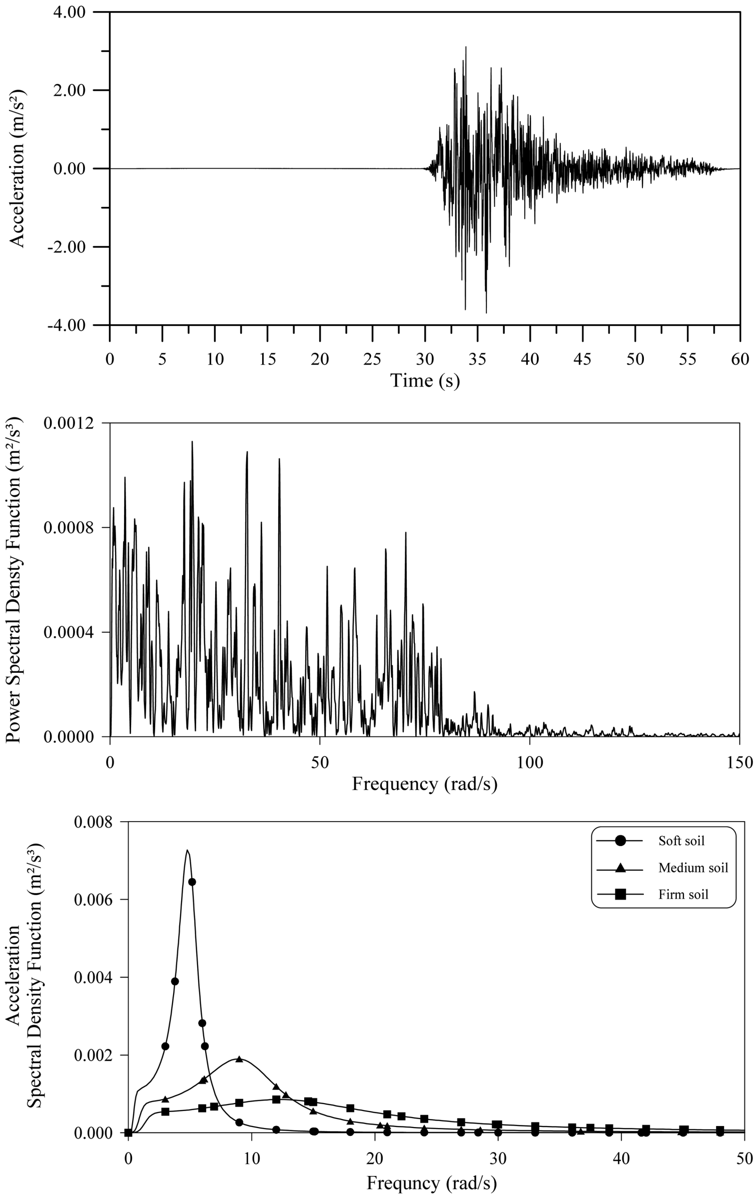

Fig. 2 SKR090 component of Sakarya station of the 1999 Kocaeli earthquake: (a) acceleration time history (b) power spectral density function (c) acceleration spectral density function for different soil types

1.09 and 2.78, respectively (Zerva 1991). Adanur *et al.* (2003) observed that the correlation function proposed by Harichandran and Vanmarcke (1986) gives the largest response values through four different correlation functions, namely Harichandran and Vanmarcke, Abrahamson, Hindy and Novak and Uscinski. This is because in this study the correlation function proposed by Harichandran and Vanmarcke (1986) is used.

The wave-passage effect resulting from the difference in the arrival times of waves at support points is defined as

$$\gamma_{lm}(\omega)^{w} = e^{i(-\omega d_{lm}^{L}/v_{app})} \tag{26}$$

where v_{app} is the apparent wave velocity and d_{lm}^{L} is the projection of d_{lm} on the ground surface along the direction of propagation of seismic waves. The apparent wave velocities employed in this study are selected as 300, 800 and 2000 m/s for soft, medium and firm soil conditions, respectively.

The site-response effect due to the differences in the local soil conditions is obtained as

$$\gamma_{lm}(\omega)^{s} = e^{i(\tan^{-1}(\mathrm{Im}(H_l(\omega)H_m(-\omega))/Re(H_l(\omega)H_m(-\omega))))} \tag{27}$$

where $H_l(\omega)$ is the local soil frequency response function representing the filtration through soil layers.

7. Numerical example

7.1 Description of the bridge

In order to investigate the stochastic response of non-isolated and isolated bridges, a two-dimensional analytical model used by Der Kiureghian *et al.* (1997) is selected as numerical examples. The selected highway bridge and its finite element models are created in Fig. 3. The bridge has uniform mass and stiffness properties along its continuous deck with a cross section. Its four identical columns with circular cross section, which diameter is 2.50 m and elastic modulus of 32E6 kN/m^2, have fixed supports at the bottom. These supports are situated on soft, medium and firm soil conditions. It is accepted that the amplitudes and frequency contents of the ground motion do not change, and the propagation speed of the seismic wave is constant along the firm soil. The distance between support points of A and B, B and C, C and D, D and E and E and F vary between 0-36.6 m, 36.6-109.8 m, 109.8-183.0 m, 183.0-256.2 and 256.2-292.8 m. The arrival time to each support of the selected bridge model is calculated using the relation of d_{lm}/v_{app}. For instance, for 300 m/s the arrival time to each support point is 0.0, 0122, 0.366, 0.610, 0.854 and 0.976 s, respectively. The arrival times are taken into account as 0.0 s for all support points when the apparent wave velocity is assumed infinite. This situation corresponds to uniform ground motion. The linear weight of the continuous deck is 172.50 kN/m, and its moment of inertia and elastic modulus are taken as 79.88 m^4 and 32E6 kN/m^2, respectively.

The SCFP and DCFP which are used as isolators for sliding isolation system of the selected bridge are connected between the top of the piers and the deck as shown in Fig. 3. The bridge is isolated with two isolators at each abutment and pier location for a total 12 isolators. The isolators are directly located on the cap beam above the circular columns at the bents. The bearings are installed at the tops of the piers as two bearings per pier and modelled as a link element with the radius and the coefficient of friction on the concave surfaces. The horizontal input is assumed to travel across the bridge from left to right side with finite velocities of 300, 800 and 2000 m/s for soft (S), medium (M) and firm (F) soil conditions, respectively. The acceleration spectral density function for firm soil type is applied to each support points as an earthquake ground motion in Fig. 4. The analyses are carried out with computer program called SVEM (Dumanoglu and Soyluk 2002) which is modified to include the behaviour frictional pendulum bearings. The first 15 modes and 5% of damping ratio are selected for the stochastic response analysis. The first 5 modes are given in Table 2.

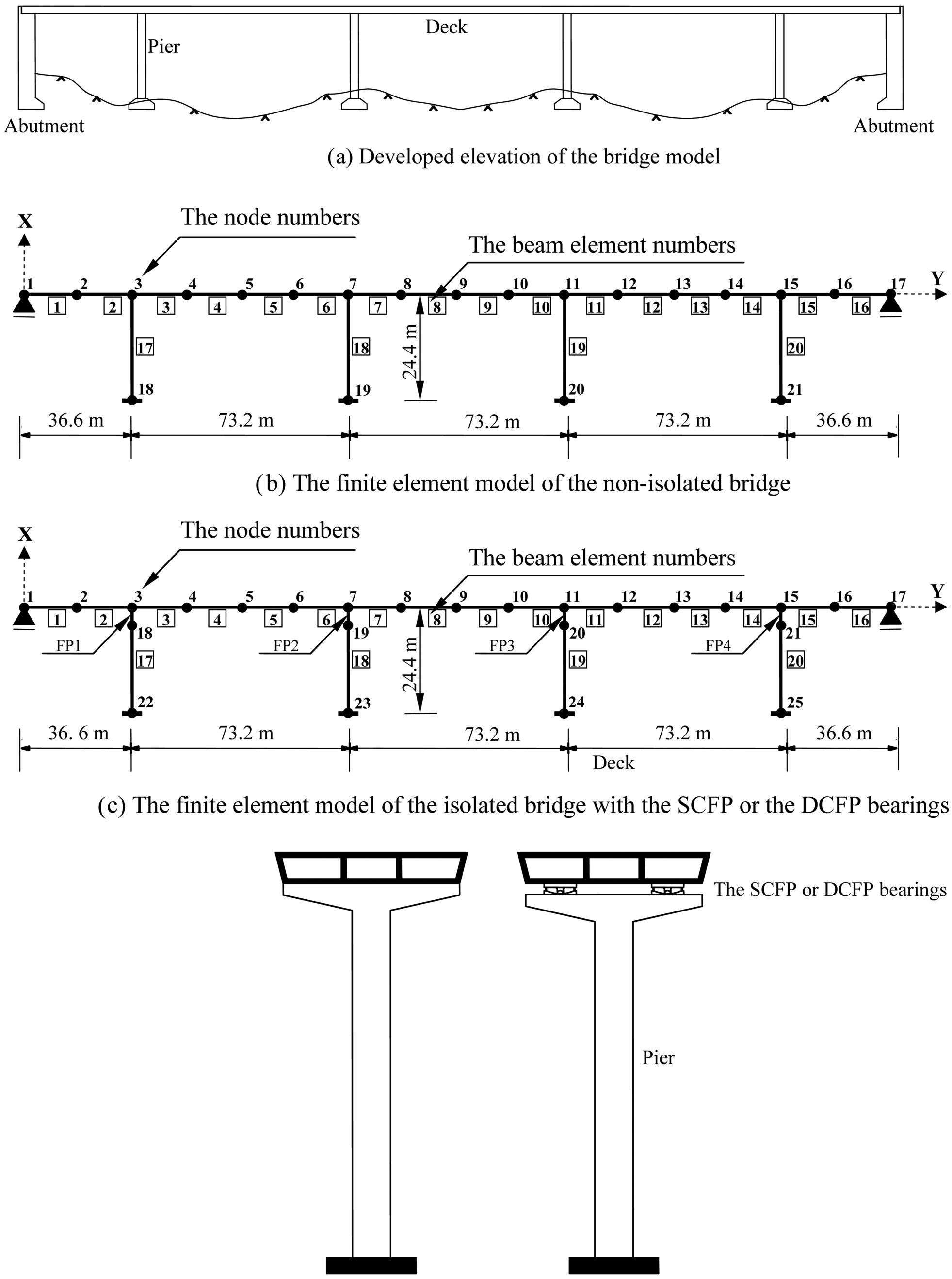

Fig. 3 The selected bridge and its finite element models

Stochastic analyses of the non-isolated and the isolated bridges are performed for spatially varying earthquake ground motion by taking into account the incoherence, the wave-passage, and the site-response effects. For this purpose, three different soil conditions are considered for the bridge model in Fig. 4. These soil conditions are FMSSMF, FMMMSS and SMFFMS.

Table 2 Vibration period of the isolated and non-isolated bridges

	Period (sec)				
Mode number	1	2	3	4	5
Non-isolated bridge	1.193	0.815	0.685	0.579	0.274
Isolated bridge with the SCFP	2.383	1.031	0.707	0.597	0.303
Isolated bridge with the DCFP	2.850	1.024	0.768	0.596	0.302

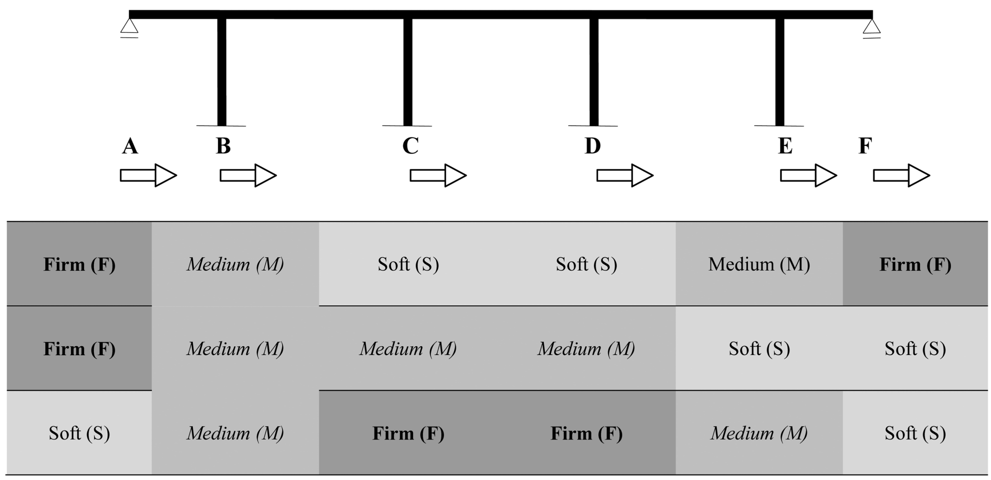

Fig. 4 The bridge system subjected to spatially varying earthquake ground motions for different soil conditions

For instance, FMSSMF: The bridge has six supports and these supports are assumed to be founded on FMSSMF. Herein F, M and S denote firm, medium and soft soil conditions, respectively. It is considered loss of coherency between support excitations and wave passage and homogeneous soil conditions ($\gamma_{lm}(\omega)^i \neq 1, \gamma_{lm}(\omega)^w \neq 1, \gamma_{lm}(\omega)^s \neq 1$) where the bridge is supported on these soils.

7.2 Mean of maximum values of response components

Mean of maximum values of horizontal deck responses calculated for different soil condition sets

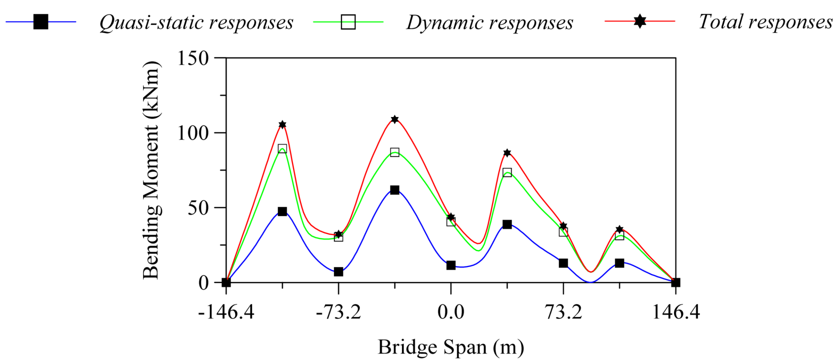

Fig. 5 Mean of maximum bending moments of the deck of the isolated bridge with DCFP (FMSSMF)

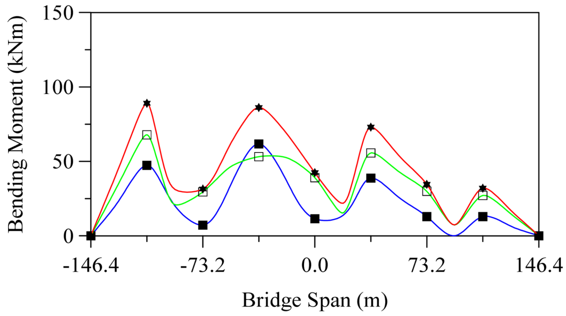

Fig. 6 Mean of maximum bending moments of the deck of the isolated bridge with SCFP (FMSSMF)

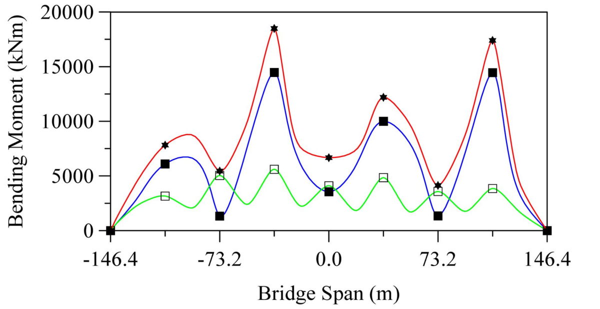

Fig. 7 Mean of maximum bending moments of the deck of the non-isolated bridge (FMSSMF)

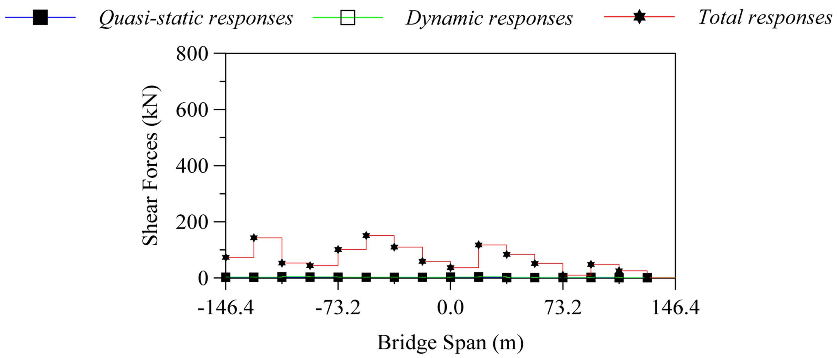

Fig. 8 Mean of maximum shear forces of the deck of the isolated bridge with DCFP (FMSSMF)

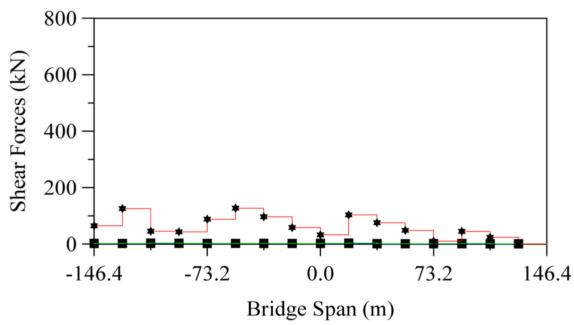

Fig. 9 Mean of maximum shear forces of the deck of the isolated bridge with SCFP (FMSSMF)

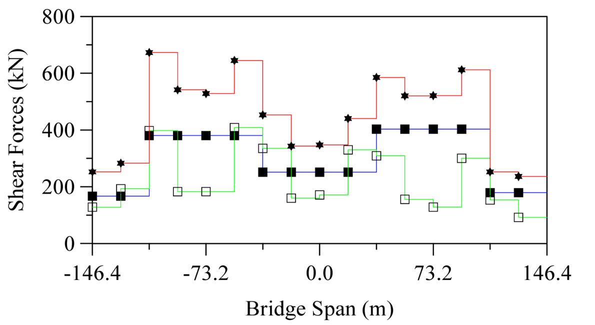

Fig. 10 Mean of maximum shear forces of the deck of the non-isolated bridge (FMSSMF)

defined as FMSSMF, FMMMSS and SMFFMS are compared for quasi-static, dynamic and total responses. Mean of maximum quasi-static, dynamic and total bending moments of deck of the non-isolated and isolated bridges calculated for several defined above cases are compared in Figs. 5-7, 14-16 and 23-25. The bending moments of deck of the non-isolated and isolated bridge obtained for the defined soil conditions set are larger than those of MMFFMM condition. The bending moments of the deck of the isolated bridge are smaller almost four times than those of non-isolated bridge with the SCFP and the DCFP. Due to seismic isolation of the bridge with the SCFP and DCFP, the

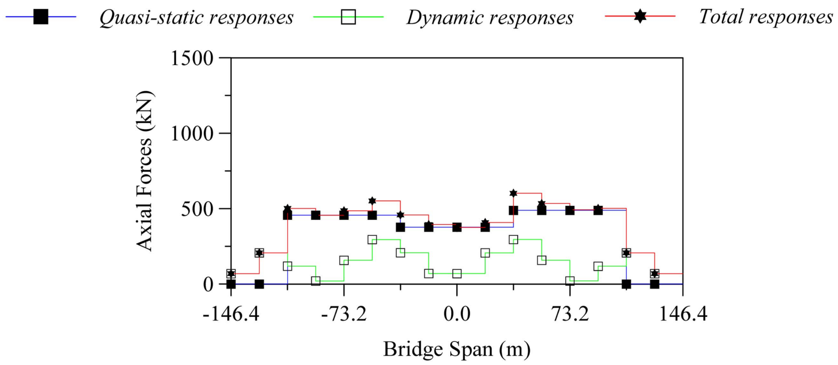

Fig. 11 Mean of maximum axial forces of the deck of the isolated bridge with DCFP (FMSSMF)

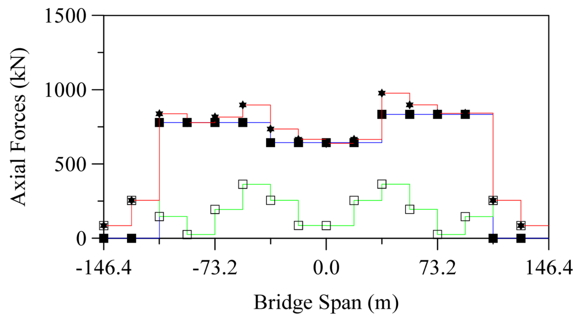

Fig. 12 Mean of maximum axial forces of the deck of the isolated bridge with SCFP (FMSSMF)

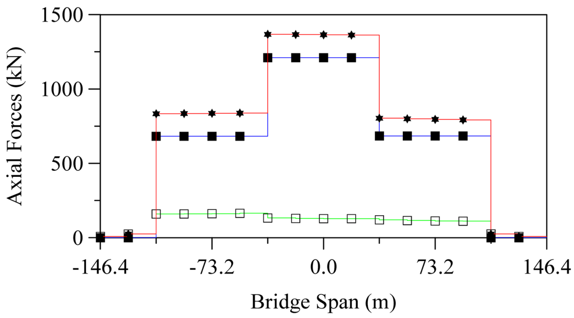

Fig. 13 Mean of maximum axial forces of the deck of the non-isolated bridge (FMSSMF)

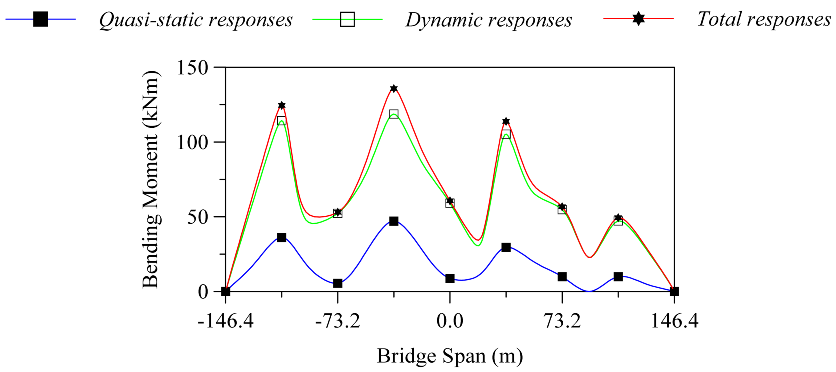

Fig. 14 Mean of maximum bending moments of the deck of the isolated bridge with DCFP (FMMMSS)

bending moments are considerably decreased. Additionally, the changing of the local soil conditions at the support points of the bridges affects response values of both the non-isolated and the isolated bridges. Differences between the soil conditions at the bridge support are increased; the responses on the deck are increased for the non-isolated bridge. But, the issue for the isolated bridge are not the same as the non-isolated bridge, the responses on the isolated deck has little changes.

Mean of maximum shear forces of the deck of non-isolated and isolated bridge are given in Figs.

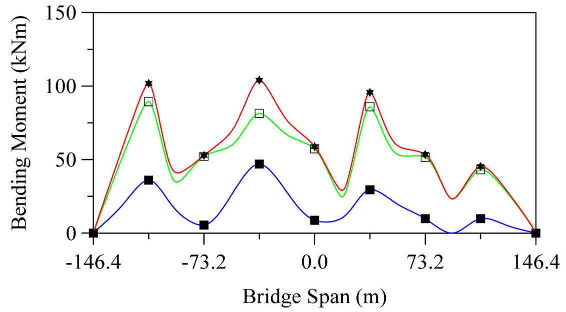

Fig. 15 Mean of maximum bending moments of the deck of the isolated bridge with SCFP (FMMMSS)

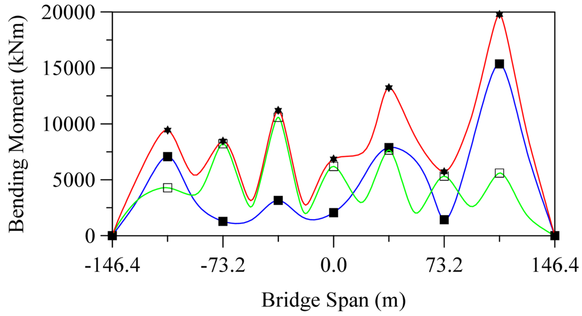

Fig. 16 Mean of maximum bending moments of the deck of the non-isolated bridge (FMMMSS)

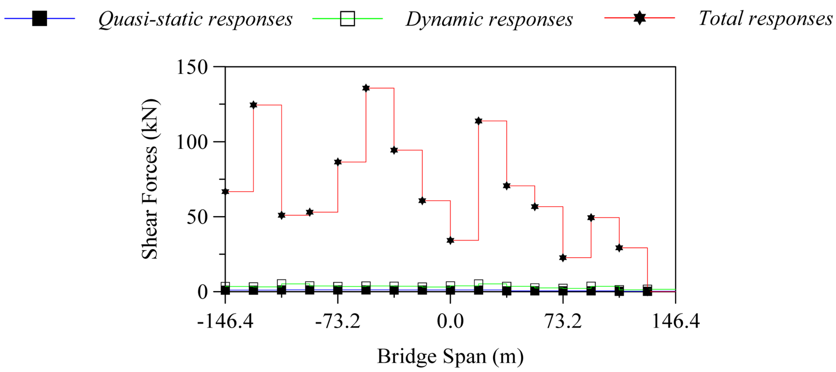

Fig. 17 Mean of maximum shear forces of the deck of the isolated bridge with DCFP (FMMMSS)

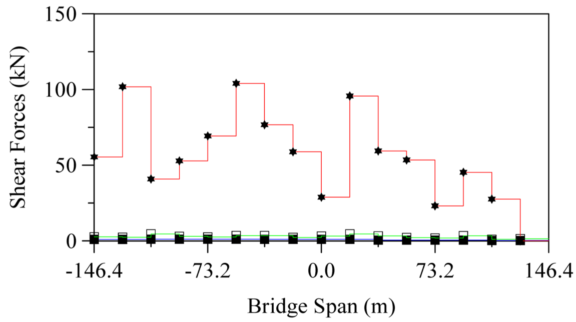

Fig. 18 Mean of maximum shear forces of the deck of the isolated bridge with SCFP (FMMMSS)

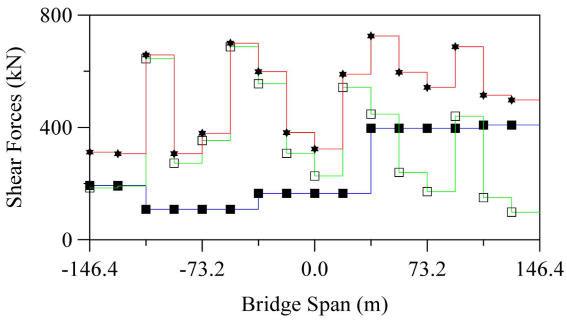

Fig. 19 Mean of maximum shear forces of the deck of the non-isolated bridge (FMMMSS)

8-10, 17-19 and 26-28. These figures show that shear forces, which occur on the deck of bridge, are significantly decreased by using isolation systems such as the SCFP and the DCFP bearings. Therefore, it is obvious that isolation of bridges to severe ground motion is required. The similar variation is also observed for the axial forces of deck of non-isolated and isolated bridges in Figs. 11-13, 20-22 and 29-31. The reduction of the deck axial forces obtained for the isolated model with the SCFP and the DCFP is obvious, if the axial forces are compared with those obtained for the

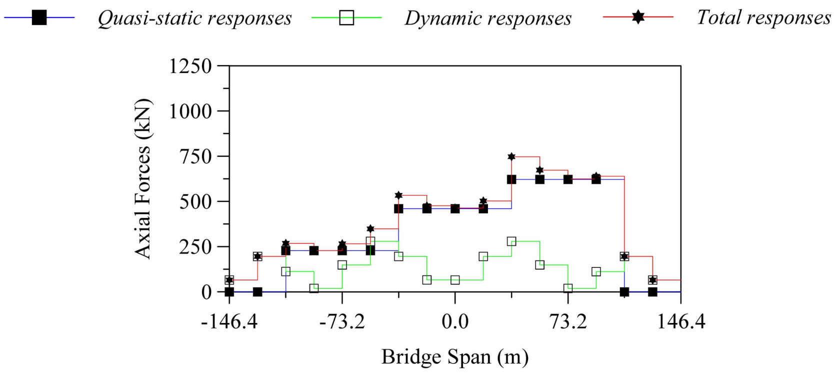

Fig. 20 Mean of maximum axial forces of the deck of the isolated bridge with DCFP (FMMMSS)

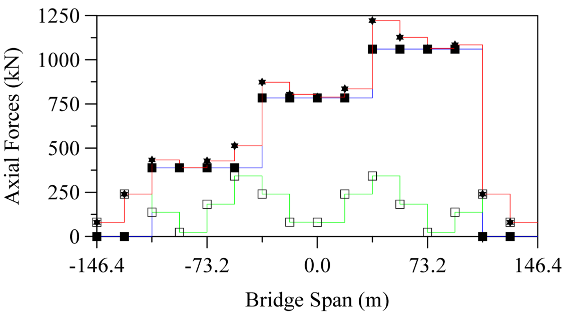

Fig. 21 Mean of maximum axial forces of the deck of the isolated bridge with SCFP (FMMMSS)

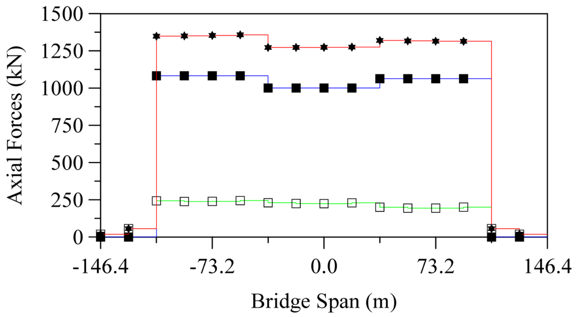

Fig. 22 Mean of maximum axial forces of the deck of the non-isolated bridge (FMMMSS)

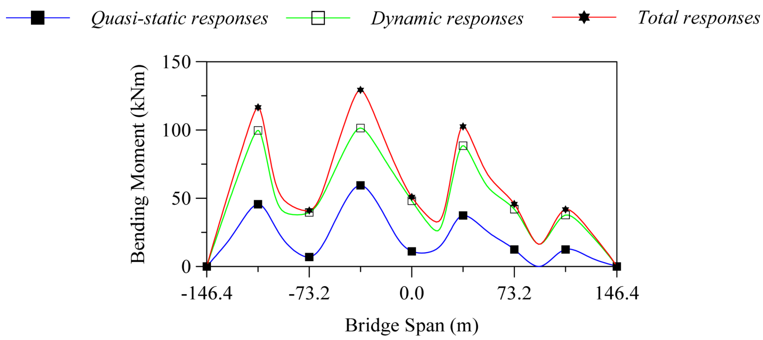

Fig. 23 Mean of maximum bending moments of the deck of the isolated bridge with DCFP (SMFFMS)

non-isolated bridge model. Significant reduction of the axial forces is provided at the connection points between the deck and piers. However, at the nodal points located at the middle of the deck, the axial forces obtained for the isolated bridge models with the SCFP and the DCFP are very close to each other.

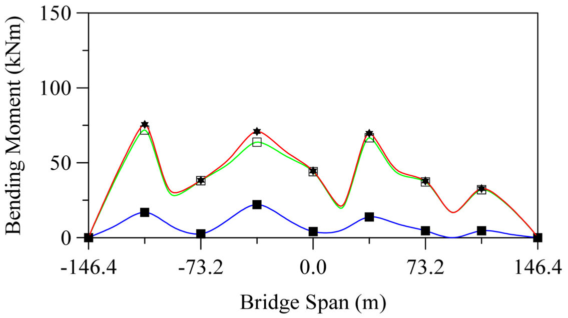

Fig. 24 Mean of maximum bending moments of the deck of the isolated bridge with SCFP (SMFFMS)

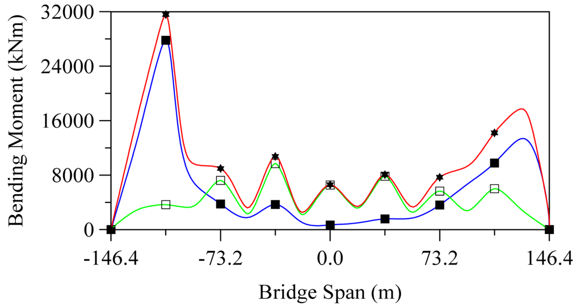

Fig. 25 Mean of maximum bending moments of the deck of the non-isolated bridge (SMFFMS)

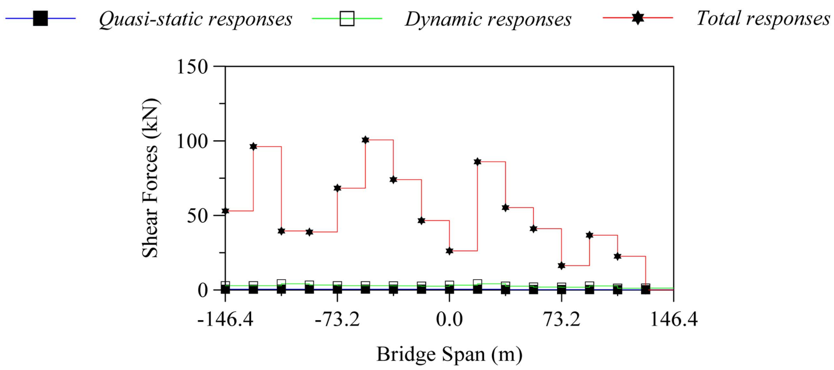

Fig. 26 Mean of maximum shear forces of the deck of the isolated bridge with DCFP (SMFFMS)

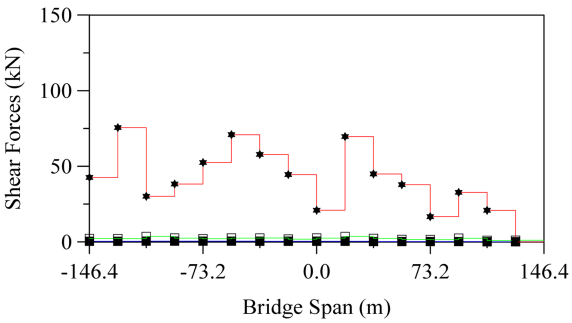

Fig. 27 Mean of maximum shear forces of the deck of the isolated bridge with SCFP (SMFFMS)

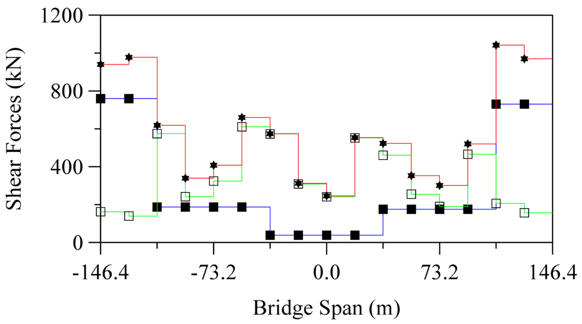

Fig. 28 Mean of maximum shear forces of the deck of the non-isolated bridge (SMFFMS)

8. Conclusions

This study outlines an investigation of the stochastic response of an isolated bridge subjected to spatially varying ground motion. The isolation devices are located at between the deck and piers as the SCFP and the DCFP bearings. Filtered white noise ground motion is considered in the analyses. The incoherence, the wave-passage and the site-response effects are taken into account in the

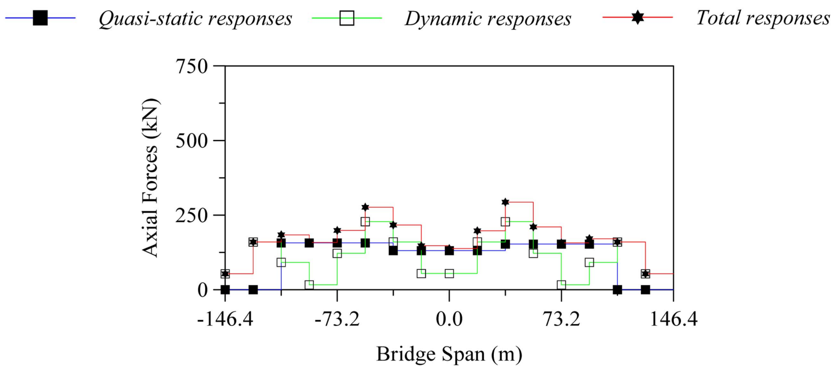

Fig. 29 Mean of maximum axial forces of the deck of the isolated bridge with DCFP (SMFFMS)

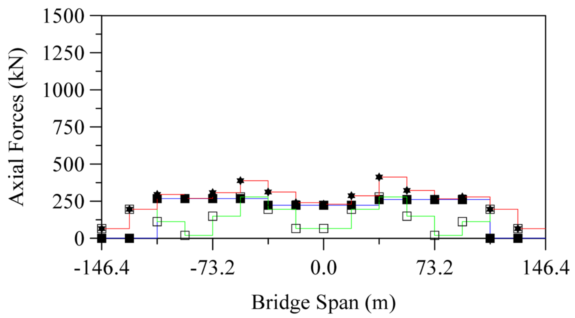

Fig. 30 Mean of maximum axial forces of the deck of the isolated bridge with SCFP (SMFFMS)

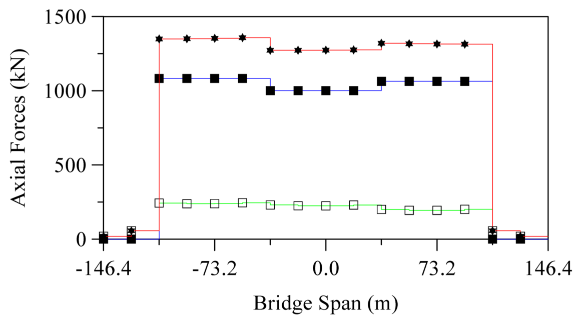

Fig. 31 Mean of maximum axial forces of the deck of the non-isolated bridge (SMFFMS)

spatially varying earthquake ground motion. The analyses are obtained for the selected the non-isolated and the isolated bridges, separately. Mean of maximum values of responses of the non-isolated and the isolated bridges are compared with each other for specialised cases of the soil conditions. The conclusions can be written as:

1. The response values carried out for spatially varying ground motion model which includes the three important effects of ground motion spatial variability are dominated by quasi-static and dynamic components.

2. The response which includes the incoherence, the wave-passage and the site-response effects obtained from the isolated bridge models with the SCFP and DCFP bearings induces large response values compared to those of the non isolated bridge model.

3. Because of the complex nature of the problem, it is difficult to make general conclusions based on this study of a single bridge model. However, as different bridge models show typically similar structural dynamics, this study mainly implies that long span bridges are sensitive to spatial variability of ground motion, and in the stochastic analysis of such type of engineering structures the incoherence, wave-passage and site-response effects should be considered.

4. Existing study on the isolated and non-isolated bridge indicates that the results obtained for the example bridge model are applicable to other bridges, as they exhibit some of the same structural dynamics. It was followed that, although the response of other bridges to different earthquakes may vary, the majority of the results presented in that study should still hold true because the bridge

models characterise the qualities of a typical bridge models. This may well be true for the results obtained from this study which is also performed on the bridge. However, the verification of the obtained results on additional bridge models should also be conducted.

5. The total response values of the non-isolated and isolated bridge carried out for the spatially varying earthquake ground motion are dominated by quasi-static and dynamic components

6. The changing of the local soil conditions at the support points affects response values of the non-isolated and isolated bridges. The more difference between the local soil conditions, the more response values take place.

7. The response values of the isolated bridge subjected to spatially varying earthquake ground motion are smaller almost four times than those of the non-isolated bridge. However, the response values of the isolated bridge show similar variation with those of the non-isolated bridge along the bridge length.

8. Usage of the DCFP bearings for seismically isolation of the bridge may reduce the response values of the bridge in accordance with the usage of the SCFP bearings.

Lastly, the aim of this paper is to investigate the effectiveness of single and double concave friction pendulum bearings on the stochastic response of isolated highway bridges when the spatially varying ground motion is considered.

References

Adanur, S., Dumanoglu, A.A. and Soyluk, K. (2003), *Stochastic analysis of suspension bridges for different correlation functions*, Proceedings of the Ninth International Conference on Civil and Structural Engineering Computing, Civil-Comp Press, Scotland.

Ates, S., Bayraktar, A. and Dumanoglu, A.A. (2006), "The effect of spatially varying earthquake ground motions on the stochastic response of bridges isolated with friction pendulum systems", *Soil Dyn. Earthq. Eng.*, **26**(1), 31-44.

Ates, S., Dumanoglu, A.A. and Bayraktar, A. (2005), "Stochastic response of seismically isolated highway bridges with friction pendulum systems to spatially varying earthquake ground motions", *Eng. Struct.*, **27**(13), 1843-1858.

Ates, S., Soyluk, K., Dumanoglu, A.A. and Bayraktar, A. (2009), "Earthquake response of isolated cable-stayed bridges under spatially varying ground motions", *Struct. Eng. Mech.*, **31**(6), 639-662.

Bilici, Y., Bayraktar, A. and Adanur, S. (2009), "Comparison of uniform and spatially varying ground motion effects on the stochastic response of fluid-structure interaction systems", *Struct. Eng. Mech.*, **33**(4), 407-428.

Clough, R.W. and Penzien, J. (1993), Dynamics of Structures, 2nd Ed, McGraw Hill Inc. Singapore.

Constantinou, M.C. (2004), Friction pendulum double concave bearing, NEES Report, available at: http://nees.buffalo.edu/dec304/FP-DC%20Report-DEMO.pdf.

Constantinou, M.C. and Papageorgiou, A.S. (1990), "Stochastic response of practical sliding isolation systems", *Probabilist. Eng. Mech.*, **5**(1), 27-34.

Der Kiureghian, A., Keshishian, P. and Hakobian, A. (1997), *Multiple support response spectrum analysis of bridges including the site-response effect and MSRS code*, Report No. UCB/EERC-97/02, Berkeley (CA): Earthquake Engineering Research Center, College of Engineering, University of California.

Der Kiureghian, A. and Neuenhofer, A. (1991), *A response spectrum method for multiple-support seismic excitations*, Report No. UCB/EERC-91/08, Berkeley (CA): Earthquake Engineering Research Center, College of Engineering, University of California.

Der Kiureghian, A. and Neuenhofer, A. (1991), *A response spectrum method for multiple-support seismic excitations*, Report No. UCB/EERC-91/08, Berkeley (CA): Earthquake Engineering Research Center, College of Engineering, University of California.

Dumanoglu, A.A. and Soyluk, K. (2002), *SVEM: a stochastic structural analysis program for spatially varying*

earthquake motions, Turkish Earthquake Foundation, TDV/KT 023-76.
Fenz, D.M. and Constantinou, M.C. (2006), "Behaviour of double concave friction pendulum bearing", *Earthq. Eng. Struct. D.*, **35**(11), 1403-1424.
Harichandran, R.S., Hawwari, A. and Sweidan, B.N. (1996), "Response of long-span bridges to spatially varying ground motion", *J. Struct. Eng.-ASCE*, **122**(5), 476-484.
Harichandran, R.S. and Vanmarcke, E.H. (1986), "Stochastic variation of earthquake ground motion in space and time", *J. Eng. Mech.-ASCE*, **112**(2), 154-174.
Hyakuda, T., Saito, K., Matsushita, T., Tanaka, N., Yoneki, S., Yasuda, M., Miyazaki, M., Suzuki, A. and Sawada, T. (2001), "*The structural design and earthquake observation of a seismic isolation building using Friction Pendulum system*", *Proceedings of the 7th International Seminar on Seismic Isolation, Passive Energy Dissipation and Active Control of Vibrations of Structures*, Assisi, Italy.
Konakli, K. and Der Kiureghian, A. (2011), "Extended MSRS rule for seismic analysis of bridges subjected to differential support motion", *Earthq. Eng. Struct. D.*, **40**(12), 1315-1335.
Lou, L. and Zerva, A. (2005), "Effects of spatially variable ground motions on the seismic response of a skewed, multi-span, RC highway bridge", *Soil Dyn. Earthq. Eng.*, **25**(7-10), 729-740.
Parka, D., Sagongb, M., Kwaka, D.Y. and Jeonga, C.G. (2009), "Simulation of tunnel response under spatially varying ground motion", *Soil Dyn. Earthq. Eng.*, **29**(11-12), 1417-1424.
Soyluk, K. and Dumanoglu, A.A. (2004), "Spatial variability effects of ground motions on cable-stayed bridges", *Soil Dyn. Earthq. Eng.*, **24**(3), 241-250.
Soyluk, K., Dumanoglu, A.A. and Tuna, M.E. (2004), "Random vibration and deterministic analyses of cable-stayed bridges to asynchronous ground motion", *Struct. Eng. Mech.*, **18**(2), 231-246.
Tsai, C.S., Chen, W.S., Chiang, T.C. and Chen, B.J. (2006), "Component and shaking table tests for full-scale multiple friction pendulum system", *Earthq. Eng. Struct. D.*, **35**(13),1653-1675.
Zayas, V., Low, S.S., Mahin, S.A. and Bozzo, L. (1989), *Feasibility and performance studies on improving the earthquake resistance of new existing building using the friction pendulum system*, Report No. UCB/EERC 89-09, Berkeley (CA): Earthquake Engineering and Research Center, College of Engineering, University of California.
Zerva, A. (1991), "Effect of spatial variability and propagation of seismic ground motions on the response of multiply supported structures", *Probabilist. Eng. Mech.*, **6**(3-4), 212-221.

CC